2024 International Nuclear Atlantic Conference – INAC 2024
Escola de Guerra Naval, Rio de Janeiro, RJ, May 6 - 10, 2024

ISBN: 978-65-594-1256-3

Application of the Convolutional Neural Network (CNN) in Image Inspection of Parts Used in Nuclear and Radioactive Installations

K. M. Tukozaki[1], F. P. Schmid[1], S. L. Somensari [1], F. A. Genezini[1], and W. A. P. Calvo[1]

[1] *mtukozaki@usp.br, fe.mecatronica@bol.com.br , somessar@ipen.br ,*
Instituto de Pesquisas Energéticas e Nucleares (IPEN / CNEN - SP)
Av. Professor Lineu Prestes 2242 - 05508-000 São Paulo, SP, Brazil

1. Introduction

In the nuclear sector, monitoring of installations and surveillance of the activities of the professionals involved must be constant and receive priority attention, with the aim of minimizing risk of workplace accidents. Despite technological updates to safety systems, nuclear reactors in operation still have serious inherent safety flaws. Additionally, many countries plan to extend the useful life of reactors beyond their original design, leading to aging and degradation of critical components. This degradation is a challenging defect to detect and can result in, serious accidents [1]. Therefore, to prolong, the life of these components and prevent degradation, their behavior must be evaluated continuously during operation [2].

The gammagraphy technique, based on the imaging produced by a radioactive source, plays a fundamental role in inspecting the interior of parts and materials, searching for defects, and enhancing the manufacturing process [3], and particularly in the nuclear sector. . There are two classifications of sources: sealed radioactive source and unsealed radioactive source. The first type, usally present in gammagraphy devices, require higher activity gamma sources than the second one, thus, requiring a lot of attention and care in relation to use and transportation by safety agencies [4].,

The use of new technologies to enhance safety, reliability and defense in depth of all parts and equipment within the nuclear/radioactive sector is highly beneficial. The artificial Inteligence is a paramount example of such new technology, being a strong trend in all regulated sectors as the nuclear and radioactive industry.[5]. One of the difficulties encountered when using imaging inspections is the large number of variables, making it challenging for operators to recognize failures. This work proposes using artificial intelligence, implemented with the Python language, for imaging analysis of pictures, to detect corrosion-type defects in sealed radioactive sources.

2. Methodology

The material used was a source holder used in industrial gammagraphy. This source holder is made with stainless steel is 175mm long, and contains oxidation that can be harmful when applied in the field. So a cell phone camera was used so that several photos of the test body were taken, and together with a library of corrosion images, it was possible to carry out an analysis (training) with the AI so that it could recognize and detect corrosion on the surface of the body.

The materials and libraries used for the program to work will be listed:

1. Font holder used in industrial gamma printing, stainless steel, shown in Fig. 1:

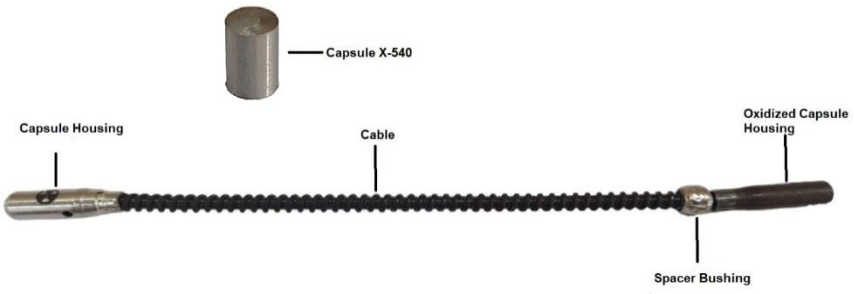

Figure 1: Font Holder.

2. Software: *Python*, version 3.11.5
    a. Libraries: *Tensorflow*, version 2.15; *Keras*, version 2.15.
3. 45 images of 1200X1600 pixels captured by the camera.
4. A camera with: 12-megapixel resolution, aperture of F2.2 [FF], field of view (FOV) of 120 degrees, sensor size of 1/2.55 inches, and pixel pitch of 1.4 µm.

The work methodology used concepts of Convolutional Neural Network (CNN) which belongs to the Deep Learning class. This Neural Network model is applied in processing and analysis for image recognition through image convolution. To apply CNN, 4 steps were performed.

The first step involved convolution of the input layer through a matrix operation with filters or kernels represented in Eq. 1, with x being the input image, S_((i,j))being the feature map and w being the kernel, in which this function is calculated in Python through the Conv2D command. The objective of this operation is to obtain the feature map, as these kernel-type filters extract features that are strongly similar between the images used for training the neural network. To carry out this step, 3X3 kernel matrices with RGB channels were used and then the non-linear activation function linear rectified linear (relu) was used, in which its mathematical operation does not activate the neurons for input values below zero, resetting the input, which makes it more The operation is efficient, as shown in Eq. 2, being calculated in Python by the command activation= 'relu'.

$$S_{(i,j)} = (x * w)_{(i,j)} = \sum_{m} \sum_{n} x(i - m, j - n) w(m,n) \tag{1}$$

$$a^{l(i.j)} = f(z^{l(i.j)}) = max\{0, z^{l(i.j)}\} \tag{2}$$

In the second stage, pooling is performed to reduce the dimensions of the generated feature maps, with the aim of simplifying the previous layers and reducing overfitting, increasing the learning capacity. There are three methods used for pooling: maxpooling, meanpooling and minpooling. In this research, maxpooling was used to return the largest value pixel (〖mr〗 _ab) during the operation together with a submatrix of dimension 2X2, according to Eq. 3. Thus, highlighting the main characteristics of the images. The command used for this operation in python was MaxPooling2D().

$$mr_{ab} = \max(m_{ij}), i \in [a, \dots (a + Q)], j \in [b, \dots (b + Q)] \tag{3}$$

Then, in the third stage, the maps resulting from the pooling operation undergo the flatten process, in which the matrix values are transformed into vectors and connected in the first layer of the Dense

Neural Network. For this, the Flatten() command was applied in Python.

In addition, in the last stage, the development of the Dense Neural Network is carried out. In this neural network, two hidden layers were developed with 128 neurons each, with the relu activation function being applied to both. In the output layer, the sigmoid activation function was used, whose operation is based on probability for binary classification, according to Eq. 4, which is calculated in Python through the activation= 'sigmoid' command [6] [7] [8] [9].

$$\varphi\big(v(i)\big) = \frac{1}{1 + e^{-v(i)}} \tag{4}$$

3. Results and Discussion

For training the Neural Network, oxidized and non-oxidized images were separated. 100 epochs were applied to train the neural network. The following result is shown in Table I, with 77% hits.

Table I: Result.

SAMPLE	PART	EXPECT RESULT	RESULT	PREVISION	CONCLUSION	SAMPLE	PART	EXPECT RESULT	RESULT	PREVISION	CONCLUSION
Porta Fonte 0	1	without oxidation	without oxidation	0,62	OK	Porta Fonte 22	2	without oxidation	without oxidation	1,00	OK
Porta Fonte 1	1	without oxidation	without oxidation	1,00	OK	Porta Fonte 23	2	without oxidation	without oxidation	0,98	OK
Porta Fonte 2	1	without oxidation	without oxidation	0,68	OK	Porta Fonte 25	3	without oxidation	with oxidation	3,92E-04	ERROR
Porta Fonte 3	1	without oxidation	without oxidation	0,72	OK	Porta Fonte 26	3	without oxidation	without oxidation	0,84	OK
Porta Fonte 4	1	without oxidation	with oxidation	0,06	ERROR	Porta Fonte 28	3	with oxidation	with oxidation	0,21	OK
Porta Fonte 5	1	without oxidation	without oxidation	1,00	OK	Porta Fonte 30	4	with oxidation	without oxidation	0,79	ERROR
Porta Fonte 6	1	without oxidation	without oxidation	0,93	OK	Porta Fonte 31	4	with oxidation	without oxidation	0,91	ERROR
Porta Fonte 7	1	without oxidation	without oxidation	0,97	OK	Porta Fonte 32	4	with oxidation	without oxidation	0,84	ERROR
Porta Fonte 8	1	without oxidation	without oxidation	0,96	OK	Porta Fonte 33	4	with oxidation	with oxidation	0,03	OK
Porta Fonte 9	1	without oxidation	with oxidation	0,36	ERROR	Porta Fonte 34	4	with oxidation	with oxidation	0,16	OK
Porta Fonte 10	1	without oxidation	without oxidation	0,54	OK	Porta Fonte 35	4	with oxidation	with oxidation	0,22	OK
Porta Fonte 11	1	without oxidation	with oxidation	0,16	ERROR	Porta Fonte 36	4	with oxidation	with oxidation	0,09	OK
Porta Fonte 12	1	without oxidation	with oxidation	0,00	ERROR	Porta Fonte 37	4	with oxidation	with oxidation	5,26E-07	OK
Porta Fonte 13	1	without oxidation	with oxidation	0,01	ERROR	Porta Fonte 38	4	with oxidation	with oxidation	0,01	OK
Porta Fonte 14	1	without oxidation	without oxidation	0,96	OK	Porta Fonte 39	4	with oxidation	with oxidation	0,01	OK
Porta Fonte 15	1	without oxidation	without oxidation	0,98	OK	Porta Fonte 40	4	with oxidation	with oxidation	2,14E-06	OK
Porta Fonte 16	1	without oxidation	without oxidation	0,98	OK	Porta Fonte 41	4	with oxidation	with oxidation	1,64E-07	OK
Porta Fonte 17	1	without oxidation	with oxidation	0,02	ERROR	Porta Fonte 42	4	with oxidation	with oxidation	5,61E-08	OK
Porta Fonte 18	2	without oxidation	without oxidation	0,92	OK	Porta Fonte 43	4	with oxidation	with oxidation	1,96E-06	OK
Porta Fonte 19	2	without oxidation	without oxidation	1,00	OK	Porta Fonte 44	4	with oxidation	with oxidation	4,27E-06	OK
Porta Fonte 20	2	without oxidation	without oxidation	1,00	OK	Porta Fonte 45	4	with oxidation	with oxidation	8,40E-09	OK
Porta Fonte 21	2	without oxidation	without oxidation	1,00	OK					hit average	77%

Subtitles for column:
1 - capsule housing
2 - capsule x-540
3 - cane
4 - Oxidized capsule housin

4. Conclusions

The preliminary results pointing out that the basis of this algorithm and this proposal can be used as basis for the development of new projects that contain specimens, algorithms, classifications, and types of defects that addressed ones in this study, but that follow the same logical principle of detecting flaws in nuclear and radioactive components, such as fretting, wear, and oxidation, among others, thus helping to optimize safety within plants.

Acknowledgements

Thanks to IPEN and CNEN to support this work and to CAPES for the scholarship

References

[1] H. Hirsch, O. Becker, M. Schneider, F. Antony, "Perigos dos reatores nucleares: riscos na operação da tecnologia nuclear no século XXI," *Estudos Avançados*, vol. 21, pp. 253–257 (2007).

[2] P. T. Gomes, J. R. B. Cruz, T. R. Mansur, "Construção de um sistema de testes de choque termico pressurizado para avaliacao da integridade estrutural de vasos de pressao de reator nuclear do tipo PWR," *International Nuclear Atlantic Conference – INAC*, Santos – Brasil, 2005, vol. 1, pp. 1-10 (2005).

[3] W. Sánchez, A. C. P. Filho, "Gamagrafia," *Instituto de Energia Atômica*, vol. 8, pp. 1–44 (1967).

[4] N. C. Rolindo, "Determinação da atividade de fontes radioativas seladas de irídio-192 em desuso," *Dissertação de Mestrado – Instituto de Pesquisas Energéticas e Nucleares de São Paulo*, pp. 1–97 (2020).

[5] R. G. da Costa, "Sistema de auxílio para o direcionamento da atenção no diagnóstico de acidentes em usinas nucleares baseado em inteligência artificial," *Dissertação de Mestrado – Instituto de Engenharia Nuclear*, Comissão Nacional de Energia Nuclear pp. 1–100 (2009).

[6] M. A. L. Vinagreiro, "Classificação baseada em espaços de camadas convolucionais de redes CNNs densas," *Dissertação de Mestrado - Escola Politécnica da Universidade de São Paulo*, pp. 1–127 (2022).

[7] R. Ruoxu, T. Hung, K. C. Tan, "A Generic Deep-Learning-Based Approach for Automated Surface Inspection," *IEEE Transactions on Cybernetics*, vol. 48, pp. 929–940 (2017).

[8] R. M. de Souza, "Classificação de falhas em ativos rotativos utilizando rede neural convolucional," *Dissertação de Mestrado - Centro Universitário Senai Cimatec*, pp. 1–85 (2020).

[9] F. Chollet, *Deep Learning with Python*, Manning Publications Co, New York & United States of America (2018).